

An Enhanced MRI Image Segmentation Approach for Brain Tumors Using SEVNet3D

Bryson Hawke

Department of Computer Science, University of Regina, Canada
bryson428@uregina.ca

Abstract: Brain tumors are a significant medical concern due to their high morbidity and mortality rates, comprising 2.4% of all human tumors. Accurate segmentation of brain tumors in magnetic resonance imaging (MRI) is crucial for effective diagnosis and treatment planning. Traditional image segmentation methods are often limited by their reliance on shallow image features and sensitivity to parameter settings. Deep learning-based segmentation techniques, while powerful, face challenges such as high computational complexity, limited accuracy, and insufficient contextual information integration. In this study, we propose an improved segmentation model, SEVNet3D, which incorporates Squeeze-and-Excitation (SE) modules to enhance the performance of the VNet architecture. The SEVNet3D model achieves better generalization and segmentation accuracy with minimal computational overhead. Despite its advantages, challenges such as the intensive workload of sample annotation and long segmentation times remain. Future work will focus on optimizing the algorithm to enable rapid segmentation and facilitate efficient diagnosis by medical professionals.

Keywords: Medical Images; SEVnet; DSC

1. Introduction

It is well known that brain tumor is one of the tumors with high morbidity and mortality, accounting for 2.4% of the incidence rate of human tumors. In general, doctors examine and diagnose patients with multimodal magnetic resonance imaging (MRI) of the brain [1]. MRI images in different modes have different imaging effects in different tumor areas [2]. Due to the influence of doctors' practical experience, personal knowledge accumulation and working hours, the analysis of image results may be quite different. Therefore, it is very important to design a precise brain tumor MRI image segmentation method. There are many types of image segmentation methods, which can be roughly divided into traditional image segmentation techniques and deep learning based image segmentation techniques. Traditional segmentation techniques mainly include edge image segmentation algorithm [3], medical image segmentation method based on threshold [4], regional growth and division merging method [5], adaptive regional growth algorithm [6], image segmentation method based on active contour model [7] and so on. The advantages of these segmentation methods are simple, efficient and easy to obtain, but the disadvantage is that only the shallow region information of the image can be used to achieve segmentation, and the segmentation results are too dependent on the specified parameters and image preprocessing. Image segmentation algorithms based on deep learning include semantic image segmentation algorithm based on full convolutional network (FCN) [8], semantic segmentation algorithm based on CNN and fully connected CRF [9], convolutional encoder architecture SegNet [10] for image segmentation, and self-encoding decoding network UNet based on expansion path and contraction path [11]. In this paper, a VNet-based SEVNet3D model

was designed to segment brain tumors.

2. Network structure and algorithm principle

This part mainly introduces SENet (Squeeze - and - Excitation Networks) module and the network proposed in this paper.

2.1 SENet module

Momenta Jie Hu team starting from the relationship between the characteristics of the channel [12], put forward the Squeeze - and - Excitation Networks (hereinafter referred to as SENet), to explicitly modeling interdependent relationship between characteristics of the channel, through the characteristics of heavy calibration, in particular, is the way through learning to automatic access to the importance of the characteristics of each channel, and then according to this useful feature importance to ascend and inhibit the characteristics of the current task would not avail much.

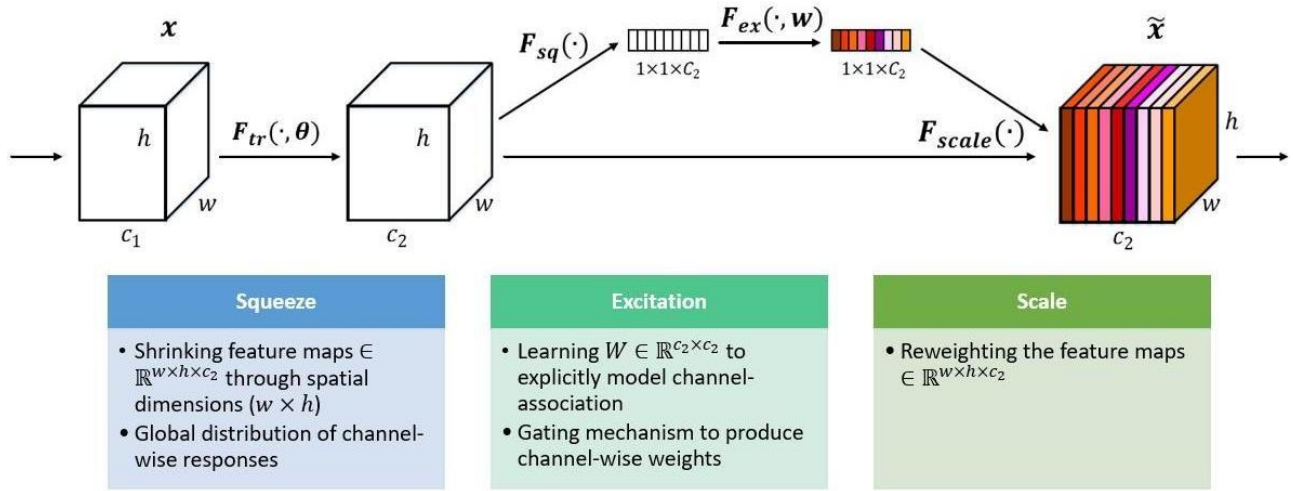


Fig1. Schematic diagram of SE module

Figure 1 is a schematic diagram of SE module. Given an input x with an number of C_1 , a feature with an specific number of C_2 is obtained through a series of convolution and other general transformations. Different from the traditional CNN, three operations are adopted to re-calibrate the previously obtained features. The first operation is Squeeze [13], which compresses the features along the spatial dimensions and turns each two-dimensional feature channel into a real number. The real number has a global receptive field to some extent [14], and the output dimension matches the input number of feature channels. The next located is the Gate [15]. The final is a Reweight operation[16]. The output weights are considered the importance of each feature channel after feature selection. The re-calibration of the original feature on the channel dimension is done using the per-channel multiplication weighting to the previous features.

2.2 SEVNet

SEVNet adds SENet module on the basis of VNet, and the network structure is shown in the Figure2.

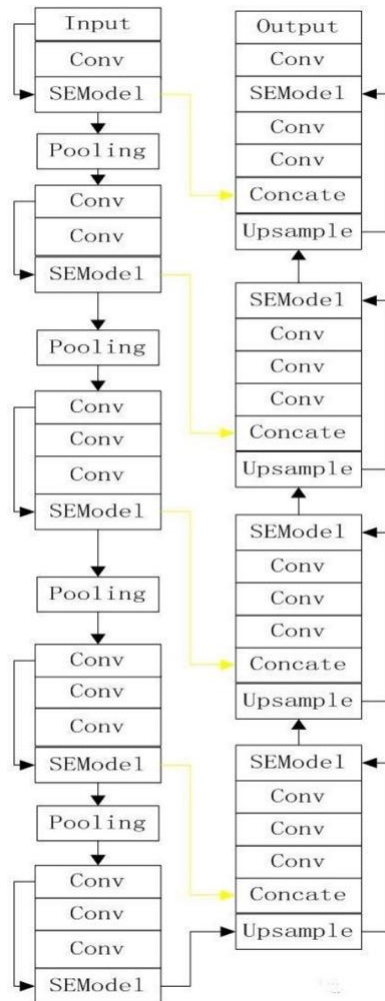


Fig.2. The network structure of SEVNet

3. Training

3.1 Pre-processing

Experimental data from MICCAI provided public data sets of brain tumors Brats2018 [17], the data set included 285 patients, by the 19 institutions use different nuclear magnetic resonance scanner, which is suitable for high grade glioma, 210 cases of 75 cases of low grade gliomas, each patient's data contains four modal (Flair, T1, T2) and T1ce MR images and real segmentation tags (Ground way), each of the MR image size is $240 \times 240 \times 155$, The Spacing was $(1 \times 1 \times 1)$ as shown in the figure3.

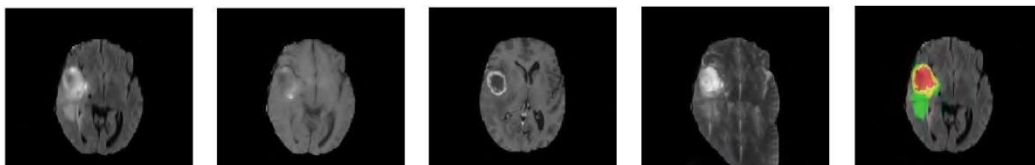


Fig.3. The size of the Spacing

The pre-processing steps are as follows:

- (1) Obtain multi-modal MR image attribute information, read the original image, display the image size, Spacing information;
- (2) Get the information of Mask images, read the Mask images, and output all label values of the Mask: 0 is the background, 1 is the gangrene area, 2 is the edema area, and 4 is the tumor enhancement area.
- (3) Multi-modal MR standardization process, BraTS18 uses MR images of Four sequences T1, T2,

Flair and T1ce. Z-Score method is adopted to standardize each modal image respectively, and the image is subdivided by the mean value and standard deviation.

(4) To prepare brain tumor segmentation data, the original MR images of 4 modal sequences were first combined to generate 3d images of 4 channels. The original image size was $(240 \times 240 \times 155 \times 1)$, and the combined size was $(240 \times 240 \times 155 \times 4)$. Second split the Mask image operations to each label image as a separate channel image, namely the size of the original image are $(240 \times 240 \times 155 \times 1)$, size is after $(240 \times 240 \times 155 \times 3)$. The non-zero value of channel 0 is the gangrene region, zero is the background region. The non-zero value of channel 2 is the swollen area. Non-zero value of channel 3 is the region of tumor enhancement, zero is the background region. Finally, the image and Mask are segmented, in other words, Patch operation is taken to generate several $(128, 128, 64)$ images and masks, and non-zero masks and corresponding images are judged and output.

3.2 The evaluation index

In order to evaluate the segmentation method proposed in this paper, using DSC (Dice Similarity Coefficient,) [18], Precision[19] and Recall[20]. The calculation formula of relevant indexes is as follows:

$$DSC = \frac{2TP}{FP + 2TP + FN}, Precision = \frac{TP}{TP + FP}, Recall = \frac{TP}{TP + FN}$$

Among them, TP and TN represent True Positive and True Negative pixels. Similarly, FP and FN represent False Positive and False Negative pixels.

3.3 Parameter setting and training

During the training, the learning rate is set to 0.001 at the initial stage, the batch size of iteration is set to 2, the training iteration period is 1000, and the Adma optimizer is used for optimization, the attenuation coefficient is 0.0001, and Early Stopping is used a strategy to determine the appropriate number of iterations.

During the training process of the improved model in this paper, the loss function of the training set and the verification set changes with the number of iterations as shown in the Figure 4. It can be seen that the loss value of the network decreases gradually with the increase of the number of iterations. When the number of training iterations reaches about 350, the network loss starts to converge and tends to be stable.

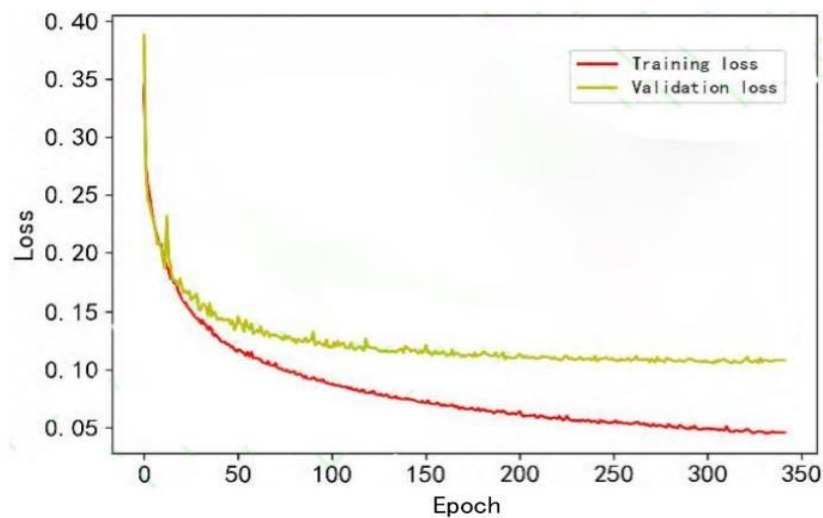


Fig. 4. The graph of loss function of training set and verification set changes with the number of iterations during training

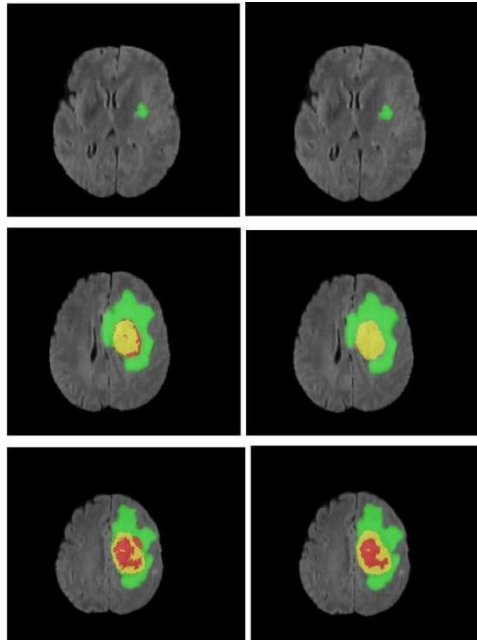


Fig.5. The result of the Segmentation

3.4 The test results

As shown in the Figure 5 below, the gold standard image is on the right and the predicted results are on the left. It can be seen that SEVNet is able to roughly divide the three regions required by the background and segmentation tasks. There is no fragmentation error segmentation in the whole tumor area. In the most difficult to segment the enhancement tumor area, it can segment the point-like, discontinuous and small tumors that are difficult to distinguish with the naked eye, and can carry out the feature sampling with high difficulty, high precision and high density.

4. Conclusion

In this paper, a SEVNet based improved MRI image segmentation method for brain tumors was proposed to address the disadvantages of the convolutional neural network segmentation method, such as high computational complexity, low accuracy, excessive depth and lack of contextual information connection. The proposed method uses SE module to easily integrate into the existing network, increase the generalization ability, improve the network performance, and the cost is very small. However, in practical application, there are still problems such as large workload of sample annotation and long time of model segmentation. According to these problems, the algorithm in this paper can be further improved to make rapid network segmentation and efficient diagnosis by doctors possible.

References

- [1] Peng Li. High Precision Integrated Navigation Algorithms for Weak Observation of Quasi-One-Dimensional Application and on Track Test[A].
- [2] Salmasi Farzin, Abraham John. Expert System for Determining Discharge Coefficients for Inclined Slide Gates Using Genetic Programming[J]. Journal of Irrigation and Drainage Engineering, 2020, 146(12).
- [3] Wang, M., Xie, Y., Liu, J., Li, A., Chen, L., Stromberg, A., ... & Wang, C. (2024). A Probabilistic Approach to Estimate the Temporal Order of Pathway Mutations Accounting for Intra-Tumor Heterogeneity. *Cancers*, 16(13), 2488.
- [4] He, W., Bao, R., Cang, Y., Wei, J., Zhang, Y., & Hu, J. (2024). Axial attention transformer networks: A new frontier in breast cancer detection. *arXiv preprint arXiv:2409.12347*.
- [5] Tohid Sardarmehni, Xingyong Song. Sub-optimal tracking in switched systems with fixed final time and fixed mode sequence using reinforcement learning[J]. *Neurocomputing*, 2021, 420.

-
- [6] Sun, D., Sui, M., Liang, Y., Hu, J., & Du, J. (2024). Medical Image Segmentation with Bilateral Spatial Attention and Transfer Learning. *Journal of Computer Science and Software Applications*, 4(6), 19-27.
- [7] Edoardo Nemni, Joseph Bullock, Samir Belabbes, Lars Bromley. Fully Convolutional Neural Network for Rapid Flood Segmentation in Synthetic Aperture Radar Imagery[J]. *Remote Sensing*, 2020, 12(16).
- [8] Merkel Christian, Hopf Jens-Max, Schoenfeld Mircea Ariel. Modulating the global orientation bias of the visual system changes population receptive field elongations.[J]. *Human brain mapping*, 2020, 41(7).
- [9] Guanghong Bin, Shuicai Wu, Minggang Shao, Zhuhuang Zhou, Guangyu Bin. IRN-MLSQR: An improved iterative reweight norm approach to the inverse problem of electrocardiography incorporating factorization-free preconditioned LSQR[J]. *Journal of Electrocardiology*, 2020.
- [10] Moghimihanjani Mehrafarin, Vaferi Behzad. A Combined Wavelet Transform and Recurrent Neural Networks Scheme for Identification of Hydrocarbon Reservoir Systems From Well Testing Signals. 2021, 143(1)
- [11] Lilach Nachum, Sangyoung Song. The MNE as a portfolio: Interdependencies in MNE growth trajectory [J]. *Journal of International Business Studies*, 2011, 42(3).
- [12] Chen Liang-Chieh, Papandreou George, Kokkinos Iasonas, Murphy Kevin, Yuille Alan L. DeepLab: Semantic Image Segmentation with Deep Convolutional Nets, Atrous Convolution, and Fully Connected CRFs. [J]. *IEEE transactions on pattern analysis and machine intelligence*, 2018, 40(4).
- [13] Badrinarayanan Vijay, Kendall Alex, Cipolla Roberto. SegNet: A Deep Convolutional Encoder-Decoder Architecture for Image Segmentation. [J]. *IEEE transactions on pattern analysis and machine intelligence*, 2017, 39(12).
- [14] Hu, J., Cang, Y., Liu, G., Wang, M., He, W., & Bao, R. (2024). Deep Learning for Medical Text Processing: BERT Model Fine-Tuning and Comparative Study. *arXiv preprint arXiv:2410.20792*.
- [15] Guofeng Qin, Qiutao Li. Pavement image segmentation based on fast FCM clustering with spatial information in internet of things [J]. *Guofeng Qin; Qiutao Li*, 2019, 78(5).
- [16] Ping Wang, Bing Han, Jie Li, Xinbo Gao. Structural Reweight Sparse Subspace Clustering[J]. *Neural Processing Letters*, 2019, 49(3).
- [17] Nalepa Jakub, Marcinkiewicz Michal, Kawulok Michal. Data Augmentation for Brain-Tumor Segmentation: A Review. [J]. *Frontiers in computational neuroscience*, 2019, 13.
- [18] Yoshinori Tanabe, Takayuki Ishida, Hidetoshi Eto, Tatsuhiro Sera, Yuki Emoto. Evaluation of the correlation between prostatic displacement and rectal deformation using the Dice similarity coefficient of the rectum[J]. *Medical Dosimetry*, 2019, 44(4).
- [19] European Society for Medical Oncology; MAP Congress 2020: Molecular Analysis for Precision oncology [J]. *NewsRx Health & Science*, 2020.
- [20] G.S. Mayer, E.R. Vrscay. Self-similarity of Fourier domain MRI data[J]. *Nonlinear Analysis*, 2008, 71(12).